



HAL
open science

Dynamic substructuring in the medium-frequency range

Christian Soize, S. Mziou

► **To cite this version:**

Christian Soize, S. Mziou. Dynamic substructuring in the medium-frequency range. *AIAA Journal*, 2003, 41 (6), pp.1113-1118. 10.2514/2.2052 . hal-00686214

HAL Id: hal-00686214

<https://hal.science/hal-00686214>

Submitted on 10 Apr 2012

HAL is a multi-disciplinary open access archive for the deposit and dissemination of scientific research documents, whether they are published or not. The documents may come from teaching and research institutions in France or abroad, or from public or private research centers.

L'archive ouverte pluridisciplinaire **HAL**, est destinée au dépôt et à la diffusion de documents scientifiques de niveau recherche, publiés ou non, émanant des établissements d'enseignement et de recherche français ou étrangers, des laboratoires publics ou privés.

Dynamic Substructuring in the Medium-Frequency Range

by

C. Soize¹ and S. Mziou²

Abstract

There are several methods in linear dynamic substructuring for numerical simulation of complex structures in the low-frequency range, that is to say in the modal range. For instance, the Craig-Bampton method is a very efficient and popular method. Such a method, based on the use of the first normal structural modes of each undamped substructure with fixed coupling interface, leads to small sized reduced matrix models. In the medium-frequency range, i.e. in the nonmodal range, and for complex structures, a large number of normal structural modes should be computed with finite element models having a very large number of degrees of freedom. Such an approach is not really efficient and generally, cannot be carried out. In this paper, we present a new approach in dynamic substructuring for numerical calculation of complex structures in the medium-frequency range. This approach is still based on the use of the Craig-Bampton decomposition of the admissible displacement field but the reduced matrix model of each substructure with fixed coupling interface is not constructed using the normal structural modes of each undamped substructure, but using the eigenfunctions associated with the first highest eigenvalues of the mechanical energy operator relative to the medium-frequency band, for each damped substructure with fixed coupling interface. The method and numerical example are presented.

¹ Professor, Laboratoire de Mécanique, Université de Marne-la-Vallée, 5 Bd Descartes, 77454 Marne-la-Vallée Cedex, France - E-mail: soize@univ-mlv.fr

² Doctorant student, Structural Dynamics and Coupled Systems Department, Office National d'Etudes et de Recherches Aérospatiales, BP 72, 92322 Chatillon Cedex, France.

Nomenclature

$A^r(\omega)$	= dynamic stiffness matrix of substructure Ω_r with free coupling interface
B, B_α	= MF narrow bands
\mathbb{B}	= MF broad band
\mathbb{C}	= set of all the complex numbers
$D^r(\omega)$	= damping matrix of substructure Ω_r with free coupling interface
\mathbb{E}_B^r	= matrix of the mechanical energy operator relative to MF band B for substructure Ω_r with fixed coupling interface
\mathbf{F}^r	= vector of the nodal external forces for substructure Ω_r
G^r	= metric matrix for substructure Ω_r with fixed coupling interface
\mathbf{G}_Σ^r	= vector of the nodal internal coupling forces for substructure Ω_r
$K^r(\omega)$	= stiffness matrix of substructure Ω_r with free coupling interface
M^r	= mass matrix of substructure Ω_r with free coupling interface
m	= number of interface coupling DOFs
N_r	= first highest eigenvalues for substructure Ω_r with fixed coupling interface
n_r	= number of DOFs for substructure Ω_r with free coupling interface
P^r	= matrix of the MF energy eigenvectors for substructure Ω_r with fixed coupling interface
\mathbf{P}^r	= MF energy eigenvector for substructure Ω_r with fixed coupling interface
\mathbf{q}^r	= vector of the generalized coordinates for substructure Ω_r with fixed coupling interface
\mathbb{R}	= set of all the real numbers
$T_{ii}^r(\omega)$	= matrix-valued frequency response function for substructure Ω_r with fixed coupling interface
\mathbf{U}^r	= vector of the n_r DOFs for substructure Ω_r
\mathbf{U}_i^r	= vector of the $n_r - m$ internal DOFs for substructure Ω_r
\mathbf{U}_j^r	= vector of the m interface coupling DOFs for substructure Ω_r
$\Delta\omega$	= bandwidth of band B
λ^r	= eigenvalue for substructure Ω_r with fixed coupling interface

Φ_{ij}^r	=	static boundary functions of the coupling interface for substructure Ω_r
Ω	=	bounded domain of the entire structure
$\Omega_r, \Omega_1, \Omega_2$	=	domains of substructures $r, 1, 2$, respectively
ω	=	angular frequency in rad/s
ω_B	=	central frequency of band B
Σ	=	coupling interface between Ω_1 and Ω_2

Introduction

In the low-frequency range, that is to say in the modal range, the dynamic substructuring methods¹⁻⁷ are efficient to calculate the linear dynamical response of complex structures modeled by the finite element method. For instance, the Craig-Bampton method¹ is very efficient and popular. This method is based on the use of the normal structural modes of each undamped substructure with fixed coupling interface allowing a reduced matrix model to be constructed. It is known that the computation and the use of the normal structural modes are not really efficient to construct such a reduced matrix model in the medium-frequency range that is to say, in the nonmodal range⁸. Recently, a method⁹ was proposed to construct a reduced matrix model in the medium-frequency (MF) range. In this paper, we present a new approach for dynamic substructuring in the MF range. This approach is similar to the Craig-Bampton method, but the normal structural modes for each undamped substructure with fixed coupling interface are replaced by the eigenfunctions associated with the first highest eigenvalues of the mechanical energy operator relative to the MF band, for each damped substructure with fixed coupling interface. This paper is mainly devoted to the presentation of a methodology.

It should be noted that the set of the eigenfunctions of the mechanical energy operator relative to an MF band of a damped structure does not coincide with the set of the normal structural modes of the associated undamped structure. From Ref. 9, it can easily be verified that these two sets coincide only (1) if the mass density of the substructure is a constant (homogeneous in mass) (generally, this property is never verified for a complex dynamical system) and (2) if the damping operator is diagonalized by the structural modes (generally, this property is not

verified for a complex dynamical system in the MF range due to the viscoelasticity behavior of the materials). If either of these two conditions is not satisfied, then this particular property does not hold: generally, these conditions are not satisfied for complex structures in the MF range and consequently, these two sets are very different (this statement which is deduced from the theory has been numerically confirmed; see for instance Ref. 10). The damping operator plays a fundamental role in the MF range due to the overlap of the normal structural modes and by their coupling by damping. The set of the eigenfunctions (which are real-valued functions) of the mechanical energy operator relative to the MF band take into account the damping operator while the set of the normal structural modes does not. Consequently, the first set is much better adapted to the MF range than the second set.

Concerning the use of the second set (normal structural modes of the associated undamped structure) in the MF range, there are two main methods.

(1) The first one consists in utilizing the normal structural modes associated with the N_{nsm} lowest eigenfrequencies. Since the MF range is considered, then N_{nsm} can be very large (several hundreds or several thousands). In this case, the strategy for analyzing the convergence is clear and consists in increasing the value of N_{nsm} . Unfortunately, such an approach can be very difficult to perform in the MF range for complex dynamical systems because N_{nsm} is very large at convergence and numerical difficulties arise. In addition, the dimension of the reduced matrix model is then large and not small.

(2) The second method consists in computing normal structural modes associated with the $M_{nsm} = N_{nsm} - N_{nsm}^0$ eigenfrequencies belonging to the MF band in which $1 \ll N_{nsm}^0 < N_{nsm}$ and where N_{nsm}^0 is the number of normal structural modes whose eigenfrequencies are lower than the MF limited band. Generally, in the MF range, the modal density can be locally high, and numerical difficulties can arise related to the convergence of any iterative algorithm used to compute the M_{nsm} normal modes. In this case, M_{nsm} is not too large, but the strategy for analyzing the convergence is not clear at all: there are two parameters for studying the convergence which are N_{nsm}^0 and M_{nsm} and the convergence is not monotonic with respect to

the couple of parameters $(N_{n.sm}^0, M_{n.sm})$. Such an approach is relatively complicate and tricky for dynamic substructuring in the medium-frequency range particularly when the number of substructures is large.

Concerning the use of the first set (eigenfunctions of the mechanical energy operator of the damped structure relative to the MF band), the eigenfunctions associated with the N_{eig} highest eigenvalues $\lambda_1 \geq \lambda_2 \geq \dots \geq \lambda_{N_{eig}} \geq \dots \rightarrow 0$ of the mechanical energy operator have to be computed. Since the trace of this mechanical energy operator is equal to $\sum_{j \geq 1} \lambda_j < +\infty$, the dominant eigensubspace can be computed using a clear and straightforward strategy for choosing (*a priori*) the order N_{eig} of the reduced matrix model adapted to the MF range⁹ of each substructure (based on the use of a simple criterion) and the convergence analysis with respect to N_{eig} is straightforward. The convergence of the iterative algorithm (subspace iteration method) used to compute the N_{eig} eigenfunctions is very fast (a few iterations). At convergence, for a given MF narrow band, dimension N_{eig} of the reduced matrix model is small. Such a set of eigenfunctions is very well adapted to the construction of the reduced matrix model in dynamic substructuring for MF range.

In order to simplify the presentation, the proposed method of dynamic substructuring in the MF range is presented utilizing the finite element discretization of the dynamical system and are deduced from the continuum formulation in viscoelastodynamics¹¹.

The first section deals with the new dynamic substructuring method adapted to the medium-frequency range for a structure constituted of viscoelastic materials (therefore, the damping and stiffness operators depend on the frequency). This new approach consists in utilizing two known results: the Craig-Bampton decomposition¹ of the admissible displacement vector space for each substructure and the construction of a reduced matrix model in the MF range introduced in Ref. 9. In the second section, the construction of the eigenfunctions of the mechanical energy operator relative to an MF band for each damped substructure with fixed coupling interface is presented. This section is mainly constituted of a short summary of a previous work⁹. Finally, in the last section, a numerical example is presented. A convergence analysis of the response

is analyzed with respect to the order of the reduced matrix model of each substructure. The validation of the dynamic substructuring method in the MF range proposed in this paper is obtained in comparing the MF dynamic substructuring results with the reference solution. The example presented has been chosen as a simple system allowing a reference solution to be constructed and allowing the presented results to be reproduced (a more complex industrial mechanical system is analyzed in Ref. 11). However, this simple system contains the required specificities: the structure is not homogeneous in mass and in stiffness and there is a significant number of normal structural modes (141 normal modes) below the MF limited broad band of analysis which itself contains a significant number of normal structural modes (108 normal modes).

Dynamic Substructuring Construction in the Medium-Frequency Range

In this paper, the formulation is written in the frequency domain ω and is presented with the finite element model^{12,13} which is deduced from the continuous formulation for three-dimensional viscoelastic media¹¹. It is assumed that the structure is constituted of two substructures (generalization to a number of substructures greater than 2 is straightforward).

Structure and Frequency Band of Analysis

We consider linear vibrations of a three-dimensional structure around a static equilibrium configuration considered as a natural state (without prestresses). At static equilibrium, the structure occupies a bounded domain Ω of \mathbb{R}^3 and is made of viscoelastic material^{8,13,14}. We are interested in the construction of the matrix-valued frequency response function of the structure in an MF narrow band B defined by $B = [\omega_B - \Delta\omega/2, \omega_B + \Delta\omega/2] \subset]0, +\infty[$, in which ω_B is the central frequency and where $\Delta\omega$ is the bandwidth. If the response has to be constructed for ω belonging to an MF broad band \mathbb{B} , then broad band \mathbb{B} is written as a finite union $\mathbb{B} = \cup_{\alpha} B_{\alpha}$ of the MF narrow bands B_{α} . The approach used for the construction of the dynamic substructuring response over MF broad band \mathbb{B} consists in constructing the response over each MF narrow band B_{α} using only the eigenfunctions of the mechanical energy operator relative to MF narrow band

B_α . Then, a concatenation of responses over bands B_α is carried out for obtaining the response on MF broad band \mathbb{B} . Below, the theory is then presented for an MF narrow band B .

Reduced Matrix Model for each Substructure and for the Structure

Structure Ω is decomposed into two substructures Ω_1 and Ω_2 whose coupling interface is Σ . The analysis is performed in MF narrow band B . We consider finite element meshes of Ω_1 and Ω_2 which are assumed to be compatible on coupling interface Σ . For $\omega \in B$ and for each substructure Ω_r with $r \in \{1, 2\}$, we introduce the \mathbb{C}^{n_r} -valued vectors $\mathbf{U}^r(\omega)$, $\mathbf{F}^r(\omega)$ and $\mathbf{G}_\Sigma^r(\omega)$ constituted of the n_r DOFs of substructure Ω_r with free coupling interface Σ , the discretized forces induced by external body and surface forces, and the discretized internal coupling forces applied to coupling interface Σ , respectively. The matrix equation for substructure Ω_r with free coupling interface Σ is then written as

$$[A^r(\omega)] \mathbf{U}^r(\omega) = \mathbf{F}^r(\omega) + \mathbf{G}_\Sigma^r(\omega) \quad , \quad (1)$$

in which symmetric $(n_r \times n_r)$ complex matrix $[A^r(\omega)]$ is the dynamic stiffness matrix of substructure Ω_r with free coupling interface Σ , defined by

$$[A^r(\omega)] = -\omega^2[M^r] + i\omega[D^r(\omega)] + [K^r(\omega)] \quad , \quad (2)$$

where $[M^r]$, $[D^r(\omega)]$ and $[K^r(\omega)]$ are symmetric $(n_r \times n_r)$ real matrices. It should be noted that the damping and stiffness matrices depend on frequency ω due to the presence of viscoelastic materials. It is recalled that the Craig-Bampton method¹ introduced for finite element models is based on the following property relative to the continuous case. The admissible displacement vector space V_r for substructure Ω_r with free coupling interface Σ can be expressed as the direct sum $V_r = V_r^\Sigma \oplus V_r^0$ of the vector space V_r^Σ of the static boundary functions relative to coupling interface Σ with the admissible displacement vector space V_r^0 for substructure Ω_r with fixed coupling interface Σ . We then propose the following approach for dynamic substructuring in the MF range. For damped substructure Ω_r with fixed coupling interface Σ , it can be proved⁹ that the set of all the eigenfunctions of the mechanical energy operator relative

to MF band B is a complete family in admissible displacement vector space V_r^0 . Consequently, the construction proposed consists in substituting the normal structural modes associated with the first lowest eigenfrequencies of undamped substructure Ω_r with fixed coupling interface Σ by the eigenfunctions associated with the first highest eigenvalues of the mechanical energy operator relative to MF band B for damped substructure Ω_r with fixed coupling interface Σ . For a fixed MF narrow band B with central frequency ω_B , the static boundary functions relative to coupling interface Σ are calculated with stiffness matrix $[K^r(\omega_B)]$ at central frequency ω_B . Let us consider the finite element model. We introduce subscript j for the m coupling DOFs and subscript i for the $n_r - m$ internal DOFs. For all ω in MF band B , we then have $\mathbf{U}_i^r(\omega) = [P^r] \mathbf{q}^r(\omega) + [\Phi_{ij}^r(\omega_B)] \mathbf{U}_j^r(\omega)$ in which $[\Phi_{ij}^r(\omega_B)]$ is the $(n_r - m, m)$ real matrix defined by $[\Phi_{ij}^r(\omega_B)] = -[K_{ii}^r(\omega_B)]^{-1} [K_{ij}^r(\omega_B)]$. The matrix $[P^r]$ is the $(n_r - m, N_r)$ real matrix whose columns are the eigenvectors associated with the N_r highest eigenvalues of a generalized eigenvalue problem $[\mathbb{E}_B^r] \mathbf{P}^r = \lambda^r [G^r] \mathbf{P}^r$ with positive-definite symmetric real matrices $[\mathbb{E}_B^r]$ and $[G^r]$ corresponding to the finite element discretization of the eigenvalue problem $\mathbf{E}_B^r \mathbf{p}^r = \lambda^{\infty,r} \mathbf{p}^r$ for the mechanical energy operator relative to band B . Linear operator \mathbf{E}_B^r is a positive-definite symmetric real trace operator⁹ which means that the positive real eigenvalues of \mathbf{E}_B^r constitute a sequence $\lambda_1^{\infty,r} \geq \lambda_2^{\infty,r} \geq \dots \rightarrow 0$ such that $\sum_{j \geq 1} \lambda_j^{\infty,r} < +\infty$ and the eigenfunctions $\{\mathbf{p}_j^r, j \geq 1\}$ constitute a complete family in V_r^0 . The reduced matrix model is obtained in taking $N_r \ll n_r - m$. The vectors of $[P^r]$ will be called the MF energy eigenvectors and are constructed in the next section. The vector $\mathbf{q}^r(\omega)$ is the \mathbb{C}^{N_r} -valued vector of the generalized coordinates. Consequently, for all ω in B , vector $\mathbf{U}^r(\omega)$ of the physical DOFs can be written with respect to $\{\mathbf{q}^r(\omega), \mathbf{U}_j^r(\omega)\}$ as

$$\begin{bmatrix} \mathbf{U}_i^r(\omega) \\ \mathbf{U}_j^r(\omega) \end{bmatrix} = \begin{bmatrix} [P^r] & [\Phi_{ij}^r(\omega_B)] \\ [0] & [I_m] \end{bmatrix} \begin{bmatrix} \mathbf{q}^r(\omega) \\ \mathbf{U}_j^r(\omega) \end{bmatrix} \quad , \quad (3)$$

in which $[I_m]$ is the (m, m) unity matrix. The $(n_r, N_r + m)$ real matrix on the right-hand side of Eq. (3) is denoted by $[H^r]$. The reduced matrix model associated with Eq. (1) is then defined by

$$[\mathcal{A}^r(\omega)] \begin{bmatrix} \mathbf{q}^r(\omega) \\ \mathbf{U}_j^r(\omega) \end{bmatrix} = \mathcal{F}^r(\omega) + \mathcal{G}_\Sigma^r(\omega) \quad , \quad \forall \omega \in B \quad , \quad (4)$$

in which $[\mathcal{A}^r(\omega)] = [H^r]^T [A^r(\omega)] [H^r]$, $\mathcal{F}^r(\omega) = [H^r]^T \mathbf{F}^r(\omega)$ and $\mathcal{G}_\Sigma^r(\omega) = [H^r]^T \mathbf{G}_\Sigma^r(\omega)$.

The reduced matrix model for the structure is usually obtained by assemblage of the substructures.

Construction of the MF Energy Eigenvectors

For a given MF narrow band B , we then have to construct the dominant eigensubspace of the generalized eigenvalue problem

$$[\mathbb{E}_B^r] \mathbf{P}^r = \lambda^r [G^r] \mathbf{P}^r \quad , \quad (5)$$

in which matrix $[\mathbb{E}_B^r]$ of the finite element discretization of the mechanical energy operator relative to band B is the positive-definite symmetric $(n_r - m, n_r - m)$ real matrix defined by⁹

$[\mathbb{E}_B^r] = [G^r] [E_B^r] [G^r]$ with

$$[E_B^r] = \frac{1}{\pi} \int_B \omega^2 \Re \{ [T_{ii}^r(\omega)]^* [M_{ii}^r] [T_{ii}^r(\omega)] \} d\omega \quad , \quad (6)$$

where \Re is the real part of complex number, $[T_{ii}^r(\omega)]^* = \overline{[T_{ii}^r(\omega)]}^T$ is the adjoint matrix and $[T_{ii}^r(\omega)] = [A_{ii}^r(\omega)]^{-1}$ exists for all ω in B . It should be noted that $[\mathbb{E}_B^r]$ depends on MF band B , but does not depend on the external excitation. The matrix $[G^r]$ is the positive-definite symmetric $(n_r - m, n_r - m)$ real matrix corresponding to the finite element discretization of the bilinear form $(\mathbf{u}, \mathbf{v}) \mapsto \int_{\Omega_r} \mathbf{u}(\mathbf{x}) \cdot \mathbf{v}(\mathbf{x}) d\mathbf{x}$ and the MF energy eigenvector $\mathbf{P}^r \in \mathbb{R}^{n_r - m}$ is the eigenvector associated with the positive real eigenvalue λ^r . The columns of $(n_r - m, N_r)$ real matrix $[P^r]$ introduced in the previous section are the eigenvectors $\mathbf{P}_1^r, \dots, \mathbf{P}_{N_r}^r$ associated with the N_r highest eigenvalues $\lambda_1^r \geq \lambda_2^r \geq \dots \geq \lambda_{N_r}^r > 0$ of the generalized eigenvalue problem. Since B is an MF narrow band, it is proved⁹ that there is a strong decrease of eigenvalues $\lambda_1^r \geq \lambda_2^r \geq \dots$ when the order of the eigenvalues is greater than a small value N_r (one dozen or a few dozens). Consequently, there exists a possibility of constructing an efficient reduced matrix model independent of the spatial excitation of the dynamical system but depending on the structural damping, that is necessary in the MF frequency range.

The construction of the dominant eigenspace of this generalized eigenvalue problem with positive matrices is performed by using the subspace iteration method¹² in which matrix $[E_B^r]$ is not explicitly calculated. An indirect procedure⁹ is used.

Numerical Example, Convergence Analysis and Validation

Defining the Dynamical System

We consider a rectangular thin plate located in the plane $(0X, 0Y)$ of a cartesian coordinate system $(0XYZ)$, in bending mode (the outplane displacement is Z). This plate is homogeneous, isotropic, simply supported, with a constant thickness $0.4 \times 10^{-3} m$, width $0.5 m$, length $1.0 m$, mass density $7800 kg/m^3$, Young's modulus $2.1 \times 10^{11} N/m^2$ and Poisson's ratio 0.29 . Two point masses of $3 kg$ and $4 kg$ are located at points $(0.2, 0.4, 0)$ and $(0.35, 0.75, 0)$, and three springs having the same stiffness coefficient $2.388 \times 10^7 N/m$ are attached normally to the plate and located at points $(0.22, 0.28, 0)$, $(0.33, 0.54, 0)$ and $(0.44, 0.83, 0)$. Consequently, the structure defined above is not homogeneous. This structure has 141 normal structural modes in the $[0, 400] Hz$ frequency band and has 108 normal structural modes in the $[400, 700] Hz$ frequency band. This structure is decomposed into two substructures Ω_1 and Ω_2 (see Fig. 1). The finite element model is constructed using 4-nodes bending plate elements. The mesh size is $0.01 m \times 0.01 m$. We have $m = 149$, $n_1 = 8989$ and $n_2 = 6009$. The total number of DOFs of the structure is $n = (n_1 - m) + (n_2 - m) + m = 14849$. For each substructure Ω_r and for a fixed narrow band B , damping matrix $[D^r(\omega)]$ is written as $[D^r(\omega)] = \theta_B [K^r]$, in which $\theta_B = 2\xi/\omega_B$ with $\xi = 0.01$.

Defining the Medium-Frequency Band and the reference solution

The reference solution of the problem is calculated over the $[0, 800] Hz$ broad frequency band by using the direct frequency-by-frequency method and without using the MF dynamic substructuring approach. Let $e(\omega) = \text{tr}\{[\mathbb{U}(\omega)][\mathbb{U}(\omega)]^*\}$ in which $[\mathbb{U}(\omega)] = [T(\omega)] [\mathbb{S}]$ is the matrix-valued frequency response function corresponding to the input DOFs defined by the $(n \times 50)$ real matrix $[\mathbb{S}]$ constituted of 0 and 1 (outplane displacements at 50 nodes uniformly

distributed in space over the structure). Figure 2 displays the graph of the function $\nu \mapsto 10 \log_{10} e(2\pi\nu)$ calculated over the $[0, 800]$ Hz broad frequency band. This figure clearly defined the medium-frequency range ($[80, 800]$ Hz) and the low-frequency range ($[0, 80]$ Hz).

MF Dynamic Substructuring

We are interested in the prediction of the response of the structure over the MF broad band $\mathbb{B} = [400, 700]$ Hz by using the MF dynamic substructuring method. The validation is obtained by comparing results with the reference solution. The MF broad frequency band is written as $\mathbb{B} = \cup_{\alpha=1}^6 B_{\alpha}$, each narrow band B_{α} having 50 Hz bandwidth. For these comparisons, we consider (1) function $\nu \mapsto 10 \log_{10} e(2\pi\nu)$ introduced in the previous subsection, (2) the frequency response function at the driven point (node 9155) of coordinates $(0.31, 0.29, 0)$, (3) the cross-frequency response function at a point (node 3235) of coordinates $(0.11, 0.49, 0)$ located in substructure Ω_1 and (4) the cross-frequency response function at a point (node 9305) of coordinates $(0.31, 0.79, 0)$ located in substructure Ω_2 (see Fig. 3).

Figures 4 and 5 correspond to the results obtained by the MF dynamic substructuring for the $[500, 550]$ Hz MF narrow frequency band. For each substructure Ω_r with fixed coupling interface, Fig. 4 displays the distribution of highest eigenvalues $\lambda_1^r \geq \lambda_2^r \geq \dots \geq \lambda_{50}^r$ of the generalized eigenvalue problem defined by Eq. (5). For each substructure, there is a strong decrease in the eigenvalues which means there exists a possibility of constructing an efficient reduced model for each substructure in this MF narrow band. It can be seen that $N_1 = 30$ and $N_2 = 25$ are acceptable values. For substructures Ω_1 and Ω_2 , dimensions N_1 and N_2 of the reduced matrix models are written as $N_1 = 5 + N$ and $N_2 = N$. Figure 5 displays the graph of the function $N \mapsto 10 \log_{10} \left\{ \int_{\mathbb{B}} e(\omega) d\omega \right\}$ which allows convergence of the response to be analyzed when the MF dynamic substructuring method is used. This graph confirms that $N_1 = 5 + 25 = 30$ and $N_2 = 25$ are reasonable values for reaching convergence.

Figures 6 to 9 correspond to the numerical results obtained by using the MF dynamic substructuring over MF broad frequency band $\mathbb{B} = \cup_{\alpha=1}^6 B_{\alpha}$. Figure 6 displays the graphs of functions $\nu \mapsto 10 \log_{10} e(2\pi\nu)$ over $[400, 700]$ Hz broad frequency band corresponding to the

MF dynamic substructuring (thick solid line) and to the reference solution (thin solid line). The small discontinuities appearing in the graphs are due to the discontinuity induced by the choice of the damping model which is constant over each MF narrow band. Figures 7 to 9 correspond to the graphs of the frequency response functions (modulus in dB and unwrap phase in radian) for the driven point (node 9155), the observation point in substructure Ω_1 (node 3235) and the observation point in substructure Ω_2 (node 9305). In each figure, the graph corresponding to the MF dynamic substructuring result (thick solid line) is compared with the reference solution (thin solid line). Figures 6 to 9 show that the method proposed gives a reasonable prediction over the MF broad frequency band.

Conclusions

We have presented a dynamic substructuring method for general damped structures modeled by the finite element method in the medium-frequency range. This method is based on the use of the Craig-Bampton method in which the normal structural modes associated with the first lowest eigenfrequencies of each undamped substructure with fixed coupling interface, is replaced by a vector basis adapted to the MF range for each damped substructure with fixed coupling interface. The reduced matrix model for each substructure is intrinsic and adapted to each MF narrow band. The method exhibits a clear strategy with respect to the truncature problems in the MF band. Therefore, all the advantages related to dynamic substructuring methods are preserved (modifications of a few substructures, response to any deterministic or random excitations, etc). In addition, the implementation of this method in existing finite element codes is very easy. The convergence of the method with respect to the main parameters has been studied. The method is convergent and the quality of the numerical predictions with the use of a reasonable numerical cost are satisfying. The extension to others dynamic substructuring methods²⁻⁷ is straightforward because the MF reduced matrix model construction of a substructure can be applied to any boundary conditions on the coupling interface : free coupling interface, hybrid coupling interface, etc. In addition, all existing techniques for reducing the number of coupling degrees of freedom can be used.

References

- ¹ Craig, R.R. and Bampton, M.C.C., “Coupling of Substructures for Dynamic Analysis”, *AIAA Journal*, Vol. 6, No. 7, 1968, pp. 1313-1319.
- ² Craig, R.R., “A Review of Time-Domain and Frequency-Domain Component Mode Synthesis Method”, in *Combined Experimental/Analytical Modeling of Dynamic Structural Systems*, Martinez D.A. and Miller A.K. eds., ASME, AMD Vol. 67, 1985, pp. 1-30.
- ³ Craig, R.R. and Chang, C.J., “On the Use of Attachment Modes in Substructure Coupling for Dynamic Analysis”, *Proceedings of the 18th Structural Dynamics and Materials Conference*, AIAA/ASME, Vol. B, AIAA Paper 77-405, 1977, pp. 89-99.
- ⁴ Jezequel, L. “A Hybrid Method of Modal Synthesis Using Vibration Tests”, *Journal of Sound and Vibration*, Vol. 100, No. 2, 1985, pp. 191-210.
- ⁵ Leung, A.Y.T., *Dynamic Stiffness and Substructures*, Springer-Verlag, New-York, 1993.
- ⁶ MacNeal, R.H. “A Hybrid Method of Component Mode Synthesis”, *Computer and structures*, Vol. 1, 1971, pp. 581-601.
- ⁷ Rubin, S. “Improved Component-Mode Representation for Structural Dynamic Analysis”, *AIAA Journal*, Vol. 13, 1975, pp. 995-1006.
- ⁸ Ohayon, R. and Soize, C., *Structural Acoustics and Vibration*, Academic Press, San Diego, London, 1998.
- ⁹ Soize, C., “Reduced Models in the Medium-Frequency Range for General Dissipative Structural-Dynamics systems”, *European Journal of Mechanics, A/Solid*, Vol. 17, No. 4, 1998, pp. 657-685.
- ¹⁰ Sakar, A. and Ghanem, R., “Mid-Frequency Vibration of Complex Uncertain System”, *Proceedings of the 8th International Conference on Structural Safety and Reliability, ICOSSAR 2001*, Newport Beach, California USA, June 17-22, 2001.
- ¹¹ Mziou, S., *Sous-structuration dynamique dans le domaine des moyennes fréquences en analyse des structures*, Thèse de Doctorat du Conservatoire National des Arts et Métiers, Paris,

November 28, 2001.

¹² Bathe, K.J. and Wilson, E.L., *Numerical Methods in Finite Element Analysis*, Prentice Hall, New York, 1976.

¹³ Zienkiewicz, O.C. and Taylor, R. L., *The Finite Element Method*, (5th edition), Butterworth-Heinemann, Oxford, 2000.

¹⁴ Truesdell, C., *Mechanics of Solids, Vol. III, Theory of Viscoelasticity, Plasticity, elastic Waves and Elastic Stability*, Springer-Verlag, 1984.

List of Figures

Fig.1 Structure constituted of a simply supported plate in bending mode, with two point masses (\bullet) and three attached springs (+), decomposed into two substructures.

Fig. 2 Reference solution: graph of the function $\nu \mapsto 10 \log_{10} e(2\pi\nu)$ for the entire structure over the $[0, 800]$ Hz broad frequency band.

Fig. 3 Driven point (node 9155) and observation points (nodes 3235 and 9305) for the frequency response function calculations.

Fig. 4 Graphs of the functions $k \mapsto \lambda_k^r$ for $k = 1, \dots, 50$ concerning the distribution of the eigenvalues of the discretized energy operator relative to the $[500, 550]$ Hz MF narrow band for substructures Ω_1 (figure on the left) and Ω_2 (figure on the right).

Fig. 5 Graph of the function $N \mapsto 10 \log_{10} \{ \int_B e(\omega) d\omega \}$ showing the convergence with respect to dimensions $N_1 = 5 + N$ and $N_2 = N$ for substructures Ω_1 and Ω_2 over the $[500, 550]$ Hz MF narrow band.

Fig. 6 Graphs of the function $\nu \mapsto 10 \log_{10} e(2\pi\nu)$ over $[400, 700]$ Hz for the MF dynamic substructuring (thick solid line) and for the reference solution (thin solid line).

Fig. 7 Frequency response function at node 9155 (driven point) in substructure Ω_1 , corresponding to the MF dynamic substructuring (thick solid lines) and to the reference solution (thin solid lines): modulus in dB (top) and unwrap phase in radian (down), the unwrap phase in radian, as a function of the frequency in Hz .

Fig. 8 Cross-frequency response function at node 3235 in substructure Ω_1 , corresponding to the MF dynamic substructuring (thick solid lines) and to the reference solution (thin solid lines): modulus in dB (top) and unwrap phase in radian (down), as a function of the frequency in Hz .

Fig. 9 Cross-frequency response function at node 9305 in substructure Ω_2 , corresponding to the MF dynamic substructuring (thick solid lines) and to the reference solution (thin solid lines): modulus in dB (top) and unwrap phase in radian (down), as a function of the frequency in Hz .

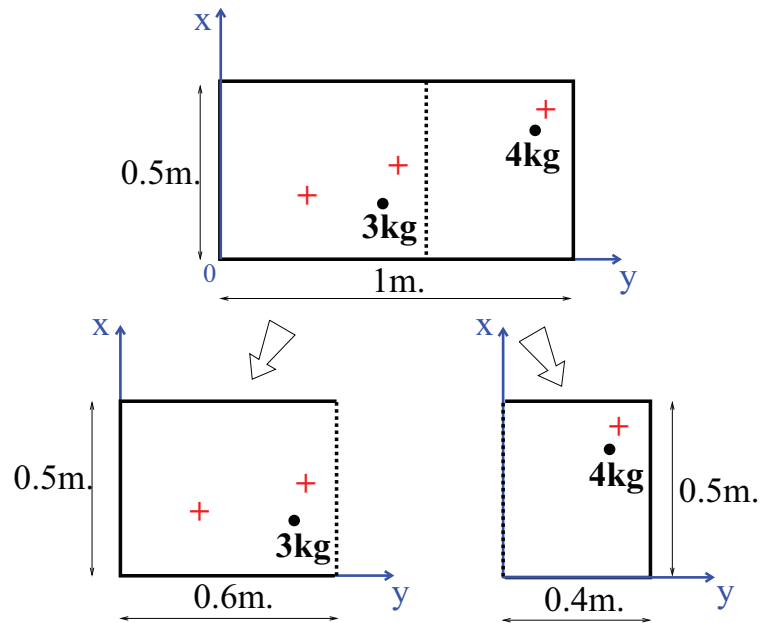


Fig.1 Structure constituted of a simply supported plate in bending mode, with two point masses (●) and three attached springs (+), decomposed into two substructures.

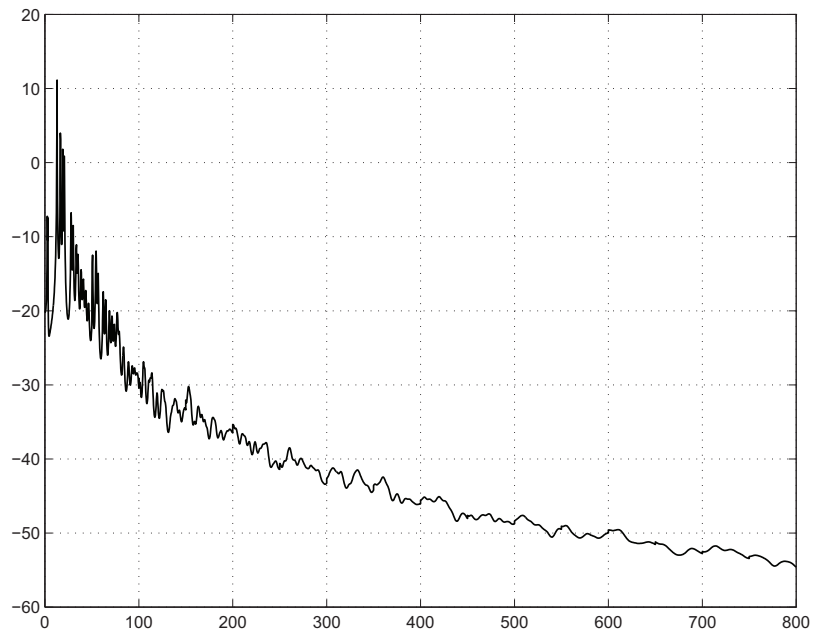


Fig. 2 Reference solution: graph of the function $\nu \mapsto 10 \log_{10} e(2\pi\nu)$ for the entire structure over the $[0, 800]$ Hz broad frequency band.

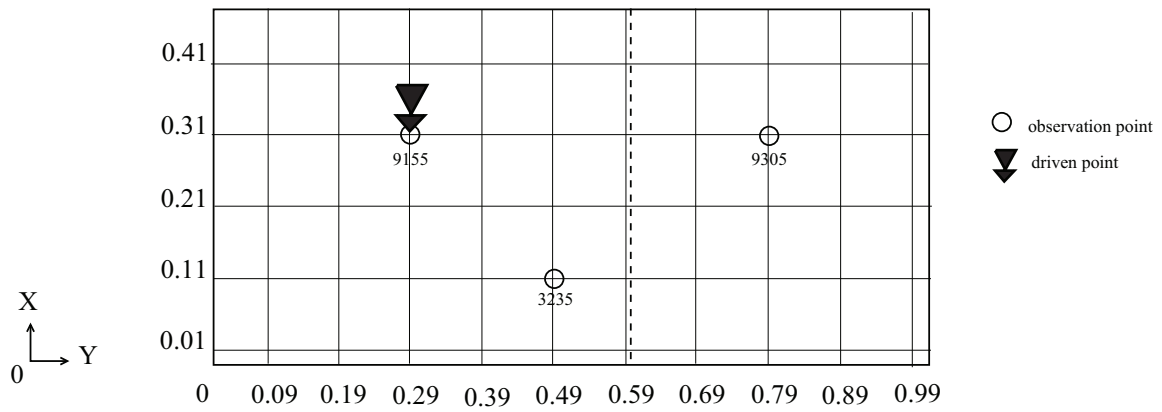


Fig. 3 Driven point (node 9155) and observation points (nodes 3235 and 9305) for the frequency response function calculations.

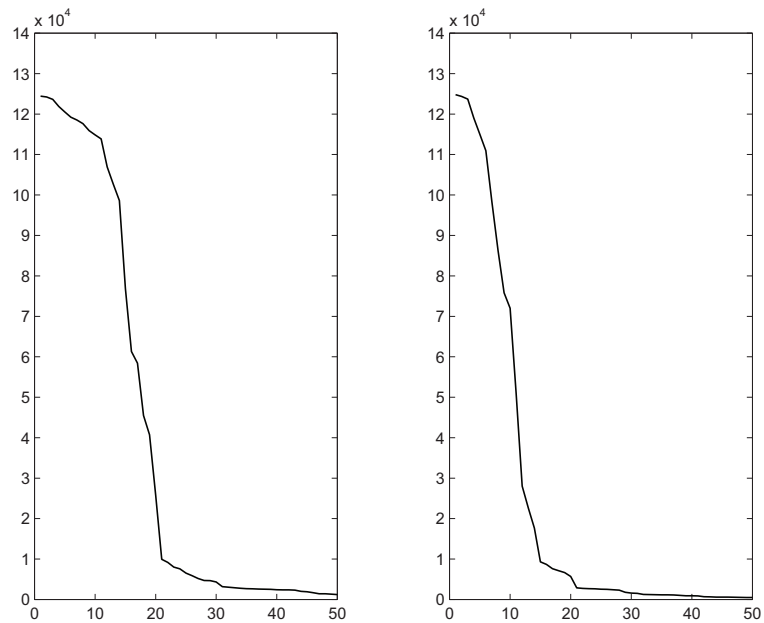


Fig. 4 Graphs of the functions $k \mapsto \lambda_k^r$ for $k = 1, \dots, 50$ concerning the distribution of the eigenvalues of the discretized energy operator relative to the $[500, 550]$ Hz MF narrow band for substructures Ω_1 (figure on the left) and Ω_2 (figure on the right).

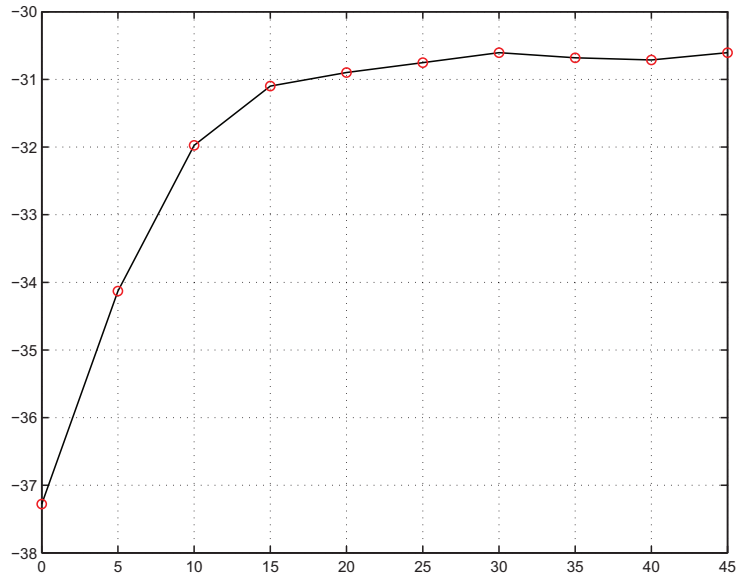


Fig. 5 Graph of the function $N \mapsto 10 \log_{10} \{ \int_B e(\omega) d\omega \}$ showing the convergence with respect to dimensions $N_1 = 5 + N$ and $N_2 = N$ for substructures Ω_1 and Ω_2 over the $[500, 550]$ Hz MF narrow band.

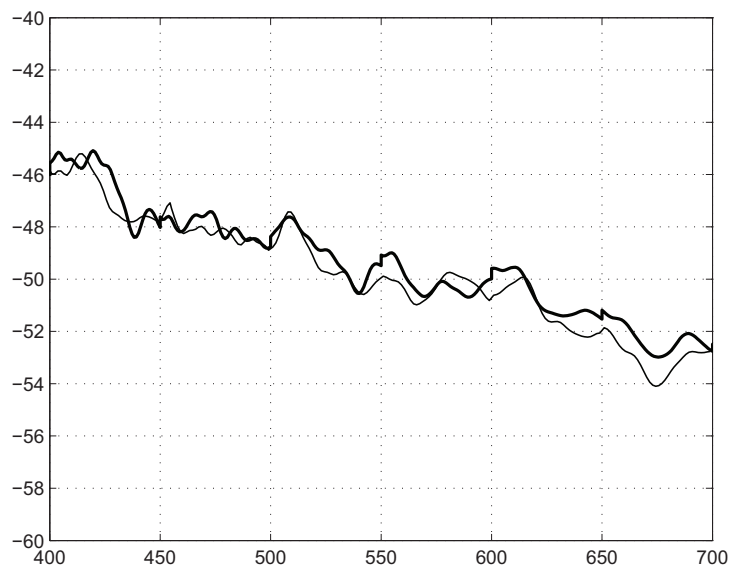


Fig. 6 Graphs of the function $\nu \mapsto 10 \log_{10} e(2\pi\nu)$ over $[400, 700]$ Hz for the MF dynamic substructuring (thick solid line) and for the reference solution (thin solid line).

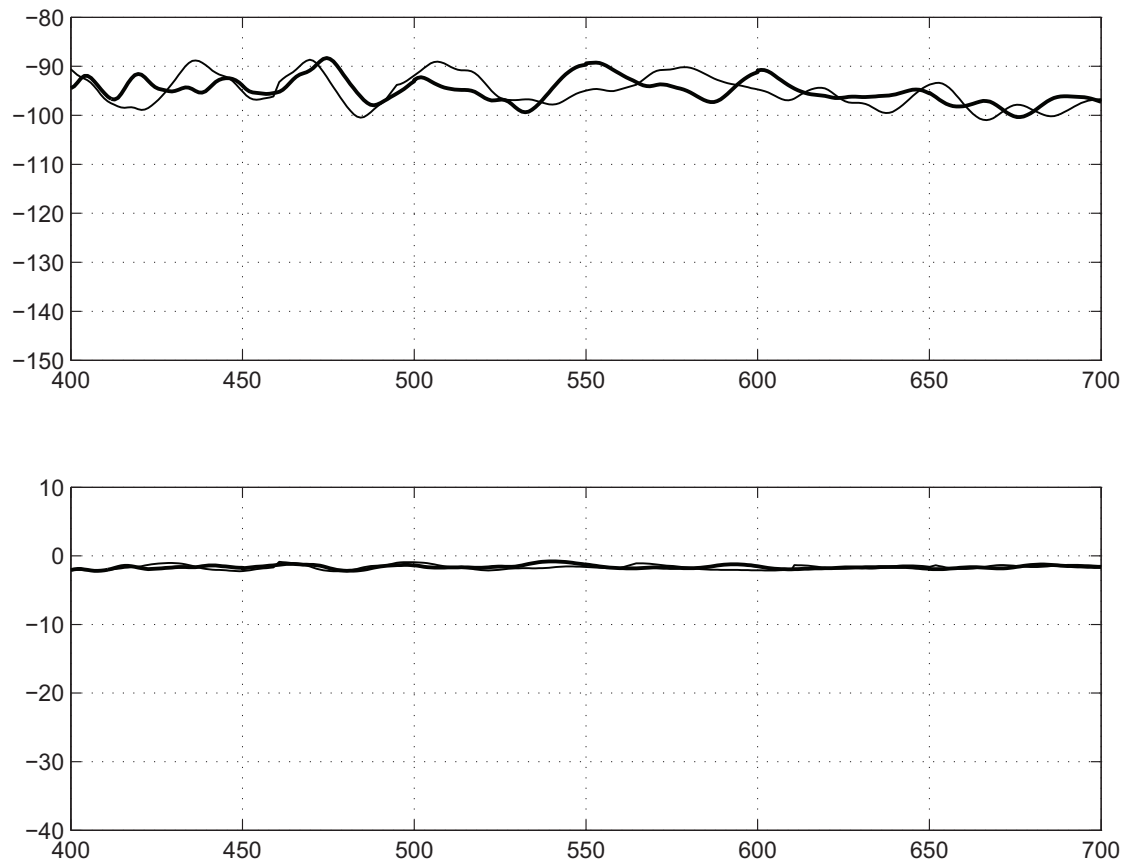


Fig. 7 Frequency response function at node 9155 (driven point) in substructure Ω_1 , corresponding to the MF dynamic substructuring (thick solid lines) and to the reference solution (thin solid lines): modulus in dB (top) and unwrap phase in radian (down), as a function of the frequency in Hz .

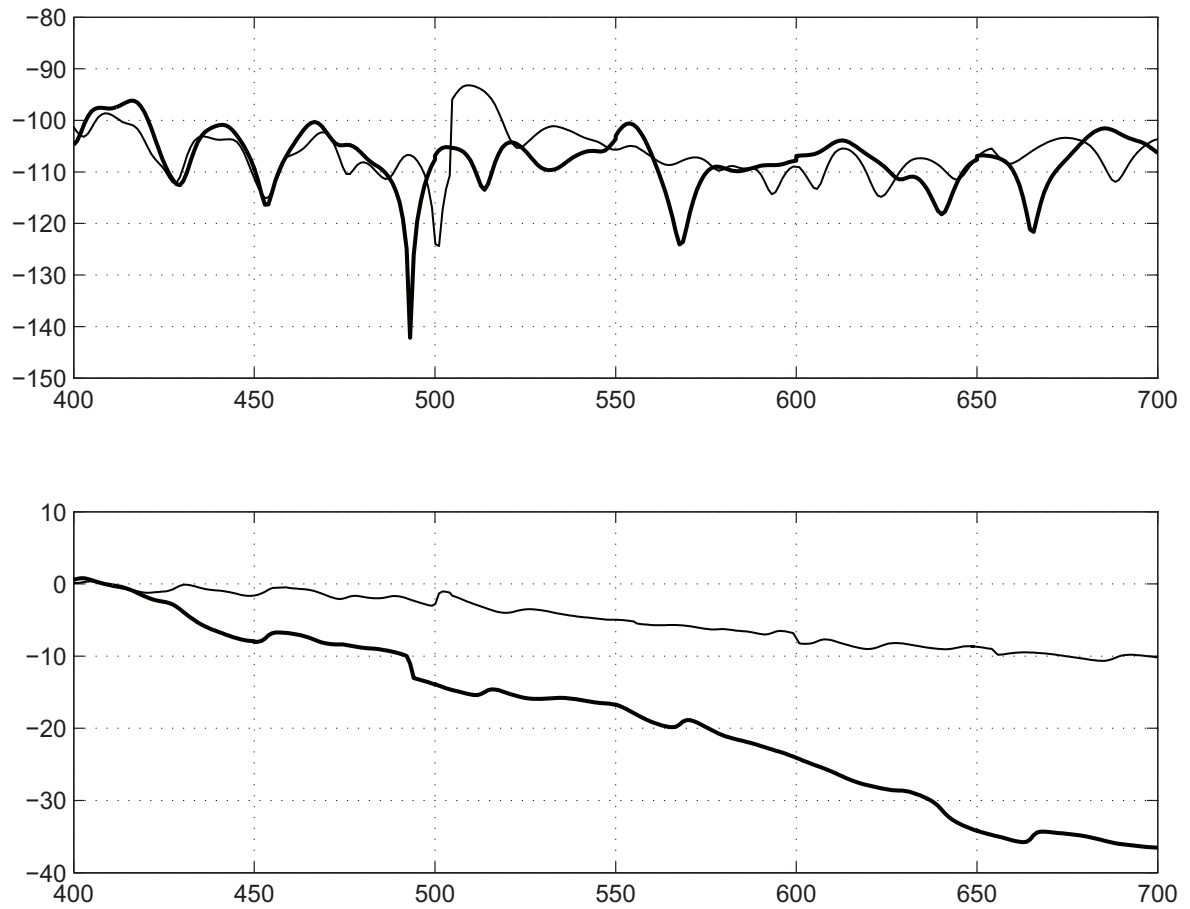


Fig. 8 Cross-frequency response function at node 3235 in substructure Ω_1 , corresponding to the MF dynamic substructuring (thick solid lines) and to the reference solution (thin solid lines): modulus in dB (top) and unwrap phase in radian (down), as a function of the frequency in Hz .

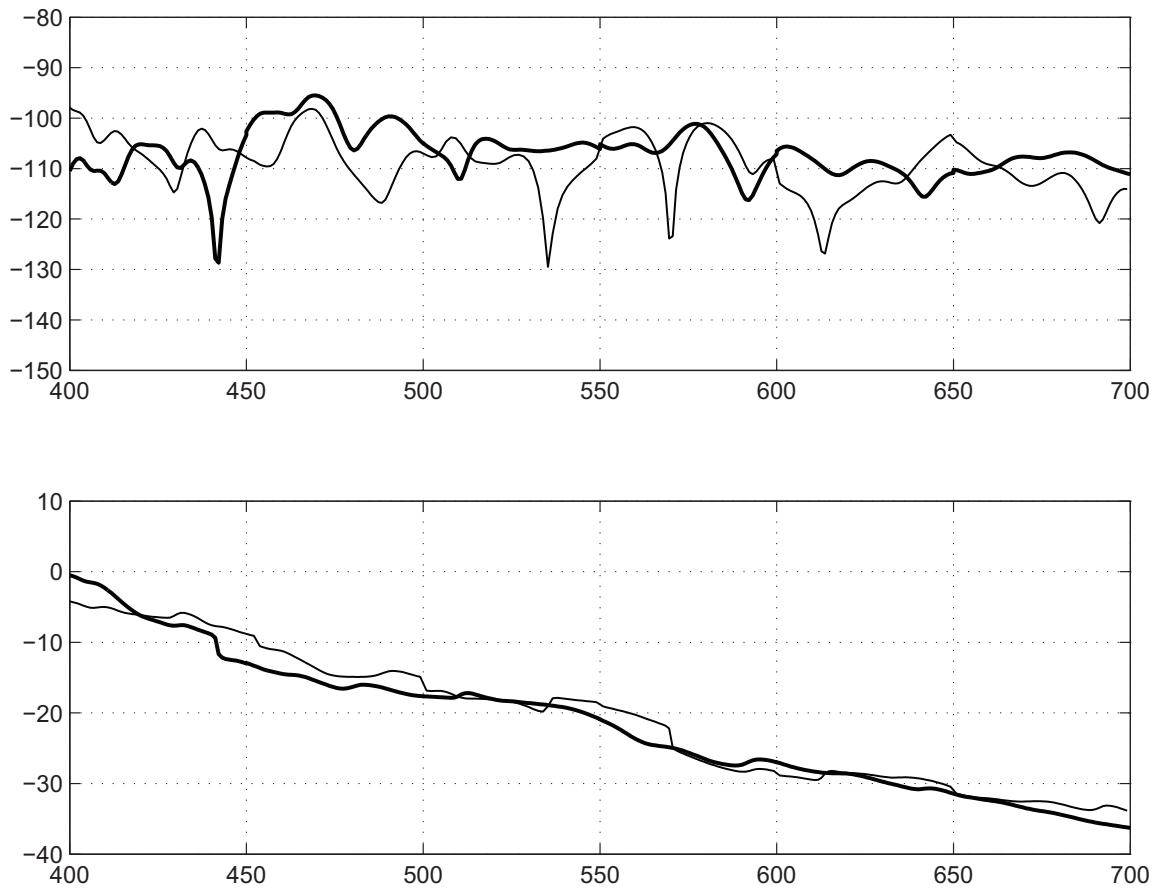


Fig. 9 Cross-frequency response function at node 9305 in substructure Ω_2 , corresponding to the MF dynamic substructuring (thick solid lines) and to the reference solution (thin solid lines): modulus in dB (top) and unwrap phase in radian (down), as a function of the frequency in Hz .